Neurosci Bull October 1, 2014, 30(5): 713–732. http://www.neurosci.cn
DOI: 10.1007/s12264-014-1463-y

·Review·

PET imaging in ischemic cerebrovascular disease: current status and future directions

Wolf-Dieter Heiss
Max Planck Institute for Neurological Research, Cologne, Germany
Corresponding author: Wolf-Dieter Heiss. E-mail: wdh@nf.mpg.de

Cerebrovascular diseases are caused by interruption or significant impairment of the blood supply to the brain, which leads to a cascade of metabolic and molecular alterations resulting in functional disturbance and morphological damage. These pathophysiological changes can be assessed by positron emission tomography (PET), which permits the regional measurement of physiological parameters and imaging of the distribution of molecular markers. PET has broadened our understanding of the flow and metabolic thresholds critical for the maintenance of brain function and morphology: in this application, PET has been essential in the transfer of the concept of the penumbra (tissue with perfusion below the functional threshold but above the threshold for the preservation of morphology) to clinical stroke and thereby has had great impact on developing treatment strategies. Radioligands for receptors can be used as early markers of irreversible neuronal damage and thereby can predict the size of the final infarcts; this is also important for decisions concerning invasive therapy in large ("malignant") infarctions. With PET investigations, the reserve capacity of blood supply to the brain can be tested in obstructive arteriosclerosis of the supplying arteries, and this again is essential for planning interventions. The effect of a stroke on the surrounding and contralateral primarily unaffected tissue can be investigated, and these results help to understand the symptoms caused by disturbances in functional networks. Chronic cerebrovascular disease causes vascular cognitive disorders, including vascular dementia. PET permits the detection of the metabolic disturbances responsible for cognitive impairment and dementia, and can differentiate vascular dementia from degenerative diseases. It may also help to understand the importance of neuroinflammation after stroke and its interaction with amyloid deposition in the development of dementia. Although the clinical application of PET investigations is limited, this technology had and still has a great impact on research into cerebrovascular diseases.

Keywords: stroke; dementia; PET; brain metabolism; brain ischemia

Introduction

The burden of cerebrovascular disease (CVD) is extremely high: in 2000 there were 15.3 million strokes world-wide, 5.5 million of which resulted in death[1]. But CVD accounts not only for 10% of all deaths; it is also the leading cause of disability in patients surviving the insult[2]. However, there exists a high variation in stroke burden and mortality, with >85% of strokes occurring in low- and middle-income countries[3]. In addition, CVD not only causes strokes, but is also associated with a high incidence of silent infarcts and microhemorrhages that lead to cognitive and behavioral changes, finally presenting as vascular dementia or cognitive impairment. Eight percent of the US population aged over 65 years experience a stroke, 8% suffer from dementia, and 17% from mild cognitive impairment of predominantly vascular origin[4].

Requirements for Brain Function

The energy demands of nervous tissue are very high and therefore sufficient blood supply to the brain must

be maintained consistently. A normal adult male's brain containing ~130 billion neurons (21.5 billion in the neocortex)[5] comprises only 2% of total body mass, yet consumes at rest ~20% of the body's total basal oxygen supplied by 16% of the cardiac output. The brain's oxygen uptake is almost entirely for the oxidative metabolism of glucose, which in normal physiological conditions is the almost exclusive substrate for its energy requirements[6]. The glucose metabolized in neurons is mainly to support cellular vegetative functions and the glucose consumption of neuronal cell bodies is essentially unaffected by functional activation, which is confined to synapse-rich regions, i.e. neuropil. The magnitudes of related increases in metabolism and blood-flow are linearly related to the frequency of action potentials in the afferent pathways regardless of whether they are excitatory or inhibitory. Increased metabolism by functional activation is mainly used to restore the ionic gradients across the cell membrane degraded by the spike activity and is rather high compared to the demand of the cell body[7]. Overall, 87% of the energy consumed is required by action potential propagation and postsynaptic ion fluxes, and only 13% is used for maintaining membrane resting potential[8].

The consequence of CVD in tissue is ischemic cell death. This results from circulatory disturbances and an insufficient blood supply leading to a complex cascade of deleterious biochemical and molecular events, which in principle are amenable to therapeutic intervention[9, 10]. Better understanding of these complex processes in ischemic stroke has improved treatment in the last decade. Pathophysiological changes that lead to irreversible tissue damage must be targets for the development of effective therapies. For therapeutic interventions in acute ischemic stroke, the concepts of the penumbra (reduced tissue perfusion and disturbed function but preserved morphological integrity) and of the time-dependent progression of irreversible tissue damage play a central role. These concepts are based on results from animal experiments, and their translation into the management of stroke patients is difficult and requires specific methods.

The Concept of the Ischemic Penumbra and Identification by Imaging

Experimental studies on the ischemic flow thresholds of brain tissue have demonstrated the existence of two critical levels of decreased perfusion: first, a level representing the flow threshold for reversible functional failure (functional threshold); and second, a lower threshold below which irreversible membrane failure and morphological damage occur. The range of perfusion values between these limits is called the "ischemic penumbra"[11], characterized by the potential for functional recovery without morphological damage, provided that local blood flow can be reestablished at a sufficient level. Whereas neuronal function is impaired immediately when blood flow drops below the threshold, the development of irreversible morphological damage is time-dependent. The interaction between severity and duration of ischemia in the development of irreversible cell damage has been established in simultaneous recordings of cortical neuronal activity and local blood flow[12]. These results complement the concept of the ischemic penumbra: the potential for post-ischemic recovery of functionally impaired cells is determined not only by the level of residual flow in the ischemic phase but also by the duration of the flow disturbance.

Autoradiographic procedures cannot demonstrate the gradual disappearance of the penumbra with increasing duration of ischemia, the progression of irreversible damage, or the recovery of functionally impaired tissue after reperfusion. To follow these pathophysiological changes, non-invasive imaging modalities, which permit repeated measurements of regional cerebral blood flow (rCBF) and regional cerebral blood volume (rCBV), as well as regional cerebral metabolic rate of oxygen ($rCMRO_2$) and of glucose (rCMRGlc), must be applied. To date, only positron emission tomography (PET) is able to quantify these variables repeatedly.

Early PET studies of stroke identified various tissue compartments within a cerebral region compromised by ischemia[13-16]. Tissue with rCBF <12 mL/100 g/min or $rCMRO_2$ <65 μmol/100 g/min at the time of measurement (usually several hours after stroke) was found to be infarcted on late CTs. Relatively preserved $CMRO_2$ is an indicator of maintained neuronal integrity in regions with CBF reduced to 12–22 mL/100 g/min. This pattern, coined misery perfusion[14], serves as a surrogate for the penumbra: it is the area with an increased oxygen extraction fraction (OEF) (to >80% from the normal value of ~40%). PET studies allow the classification of three regions

within the disturbed vascular territory: the ischemic core with a flow <12 mL/100 g/min usually showing a transition into necrosis; a penumbra region with a flow between 12 and 22 mL/100 g/min of still viable tissue but with uncertain chances for infarction or recovery; and a hypoperfused area (>22 mL/100 g/min) not primarily damaged by the reduced blood supply. The conversion of the penumbra into infarction is a dynamic process, and irreversible damage spreads from the core to its border. This process can be imaged with advanced PET equipment, by which changes in regional blood-flow and oxygen consumption have been studied after occlusion of the middle cerebral artery (MCA) in baboons and cats (reviewed in [17-19]).

In the cat, changes after MCA occlusion are immediate and severe. Sequential studies of rCBF, $rCMRO_2$, and rCMRGlc from control to the endpoint 24 h after occlusion recorded an immediate decrease in CBF within the MCA territory to <30% (Fig. 1) of control upon arterial occlusion. $rCMRO_2$ was preserved at an intermediate level and OEF was increased, indicating misery perfusion. Over time OEF decreased, reflecting progressive necrosis spreading from the core to the periphery of the ischemic territory. Reversible ischemia was studied by reopening the MCA after 60 min. If OEF remained elevated throughout the ischemic episode, reperfusion prevented large infarcts. In contrast, if the initial OEF increase disappeared during ischemia, large infarcts developed and intracranial pressure increased fatally. These experimental findings

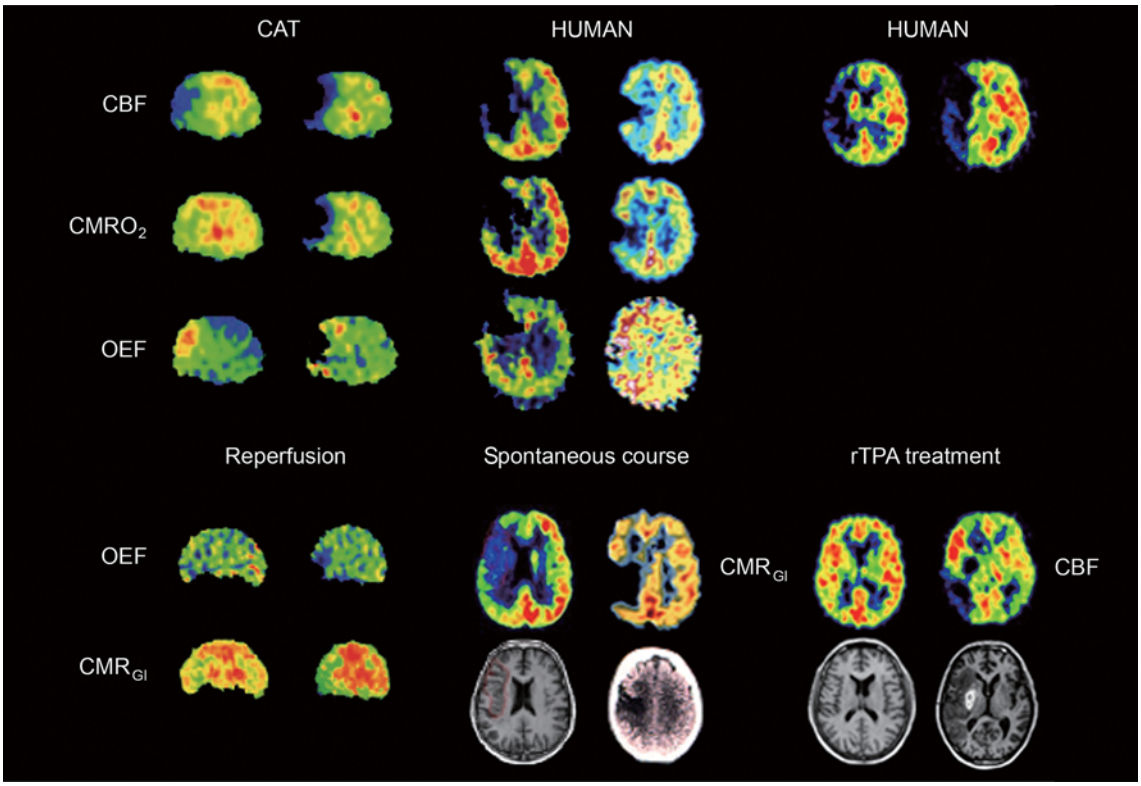

Fig.1. Sequential PET images of CBF, $CMRO_2$, and OEF after MCA occlusion in cats compared to images from patients after stroke (modified from Heiss WD. Stroke 2012[19]). Left columns: In the right cat panel, the progressive decrease of $CMRO_2$ and the reduction of OEF predict infarction and cannot benefit from reperfusion. Only if OEF is increased until the start of reperfusion can it be salvaged (left cat panel). Middle panels: in the patient, the areas with preserved OEF are not infarcted and can survive in the spontaneous course (posterior part of ischemic cortex in the left, and anterior part in the right patient as indicated on late MRI and CT). Right panels: in patients receiving recombinant tissue plasminogen activator treatment, measurements of $CMRO_2$ and OEF are not feasible, but flow determinations show the effect. If reperfusion occurs early enough and before tissue damage, tissue can be salvaged (left patient). If reperfusion is achieved too late, tissue cannot be salvaged despite hyperperfusion in some parts (right patient).

from sequential studies and clinical investigations at different time-points after the attack (Fig. 1)[20, 21] imply that the extent of the penumbra, i.e. of morphologically intact but functionally impaired tissue, depends on the time of measurement relative to the onset of ischemia. Flow measurements in the first hours after a stroke allow the identification of various tissue compartments and their contribution to the final infarct on CT/MRI. When the threshold for probable infarction was set to the conventional value of 12 mL/100 g/min and that for the upper limit of the penumbra to 18 mL/100 g/min, a large compartment of the final infarct (70%) was perfused at <12 mL/100 g/min, a level that predicts necrosis, while a smaller portion (18%) had flow values in the penumbra range (12–18 mL/100 g/min), and a fairly small compartment (12%) had perfusion at a higher level[20]. Only the tissue with CBF >12 mL/100 g/min could benefit from thrombolysis.

Non-invasive Imaging of the Penumbra

Measurement of rCBF, $rCMRO_2$, and OEF by ^{15}O-PET necessitates arterial blood sampling. A marker of neuronal integrity is needed that can identify irreversible tissue damage irrespective of the time after the vascular attack without the necessity of arterial blood sampling. The central benzodiazepine receptor ligand flumazenil (FMZ) binds to the GABA receptors abundant in the cerebral cortex. These receptors are damaged early by ischemia and indicate early neuronal loss. In cats with transient MCA occlusion, reduction in FMZ-binding predicts the size of the final infarcts, whereas preserved FMZ-binding indicates an intact cortex[17, 22]. With this tracer (Fig. 2), the pathophysiological changes early after ischemic stroke can be accurately specified: 55% of the volume of the final infarct had decreased FMZ uptake, indicating infarction in the first hours after stroke; and 21% of the final infarct had flow <14 mL/100 g/min, but FMZ uptake above the critical value, indicating penumbra tissue[17]. However, selective neuronal loss can occur in tissue outside the documented penumbra or in re-perfused penumbra areas, and this can be documented by decreased cortical FMZ-binding[23]. These results indicate the potential and the limits of therapy in acute stroke: early reperfusion cannot reverse the already-developed neuronal damage, but is crucial for salvaging the penumbra.

MR studies using diffusion and perfusion imaging might provide a differentiation between the core and the penumbra: the early diffusion-weighted imaging (DWI) lesion might define the ischemic core and adjacent critically hypoperfused tissue might be identified with perfusion-weighted imaging (PWI)[24]. Therefore, brain regions with hypoperfusion assessed by PWI but without restricted diffusion (PWI/DWI mismatch) have been assumed to represent the penumbra, but this surrogate definition has several uncertainties[25]. Several studies have been performed to validate this mismatch as a surrogate of the penumbra in the PET-derived discrimination of irreversibly damaged, critically perfused “at risk”, and oligemic “not at risk” tissue. These studies demonstrated that DWI is a rather reliable predictor of the finally infarcted tissue[26], but contains up to 25% false-positive, i.e. surviving tissue. The inaccuracy in defining the penumbra with the PWI/DWI mismatch is mainly related to the PWI, which uses variable parameters to estimate perfusion. As a consequence, the perfusion lesion size differs markedly depending on the parameters calculated[27] and is usually overestimated. Time-to-peak delays of 4 and 6 s reliably identify hypoperfused and exclude normoperfused tissue but overestimate the volume of critically perfused but salvageable tissue, i.e. the penumbra[28]. The mismatch volume in PWI/DWI as conventionally calculated therefore does not reliably reflect misery perfusion, i.e. the penumbra as defined by PET (Fig. 3). Several validation studies of various perfusion parameters calculated from PW-MRI on the flow values obtained from $H_2{}^{15}O$-PET[29, 30] resulted in corrections permitting reliable classification of critical, but potentially reversible ischemia (T_{max}, CBF, and time-to-peak). These thresholds have been implemented in recent clinical trials to improve the efficiency of therapeutic interventions for stroke[31]. With the advances of arterial spin-labelling MR techniques[32] and CT perfusion studies for the determination of cerebral perfusion[33], it will be necessary to validate the results of flow values from quantitative methods.

Detection of Hypoxic Tissue

Markers of hypoxia have been investigated with respect to their sensitivity in identifying penumbral tissue. Increased uptake of labeled nitroimidazole-derivatives is found in

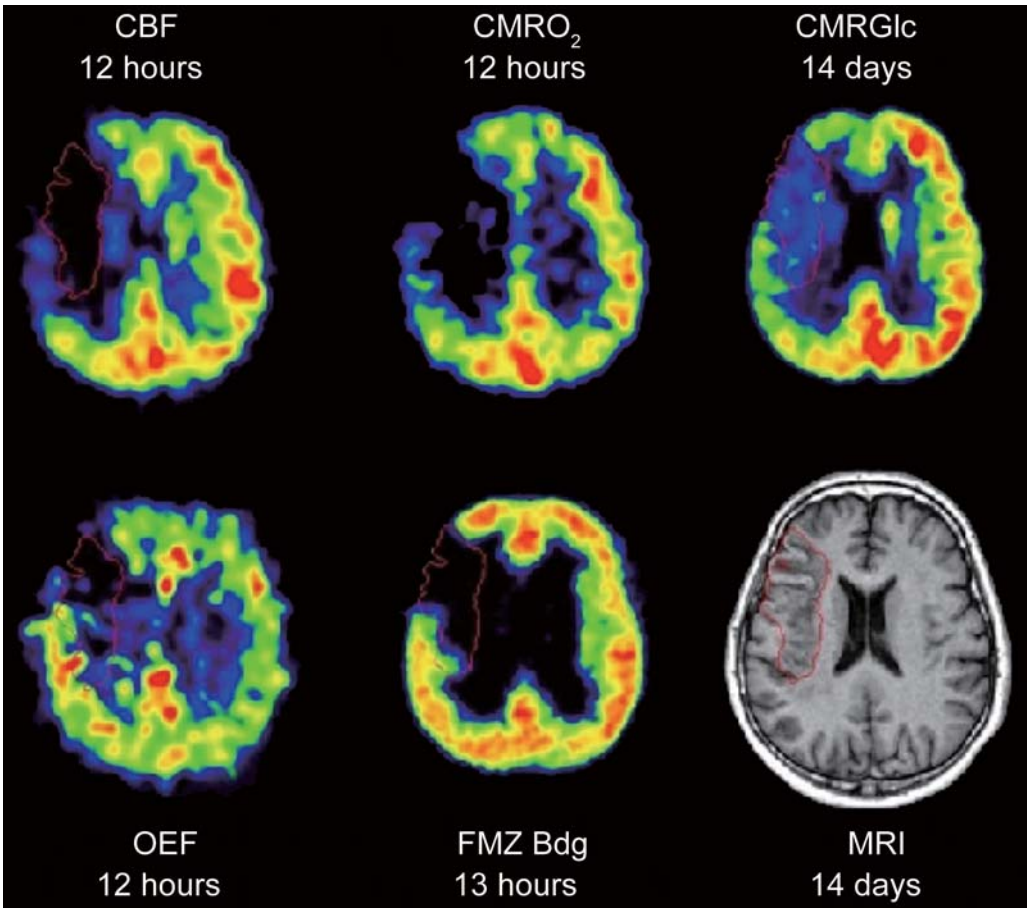

Fig. 2. Co-registered transaxial PET images at the caudate/ventricular level of CBF, steady-state FMZ binding (Bdg), and OEF at 12 h, as well as CMRGlc (glucose consumption) and MRI at 2 weeks after moderate left hemiparesis and hemihypesthesia of acute onset in a 52-year-old male patient (adapted from Heiss WD *et al.* Stroke 1998[12]). The large territorial defect is visible in all PET modalities with different extensions. The contour delineates the cortical infarct as determined on late MRI. FMZ-binding precisely predicts the extension of the final infarct, whereas CBF and FMZ distribution (as markers of perfusion) delineate a considerably larger volume of disturbed perfusion. In the cortical region outside the infarct with initially disturbed perfusion, OEF is increased, indicating preserved $CMRO_2$ at 12 h post-ictus. The permanently decreased CMRGlc in this region could be caused by neuronal loss and/or diaschisis.

the histologically-damaged ischemic core and in adjacent areas that are intact at follow up[34, 35]. The nitroimidazole-derivative misonidazole labeled with ^{18}F-fluoromisonidazole (FMISO), was first used by Yeh *et al.* in 1994[36] to investigate ischemic stroke in patients and revealed increased uptake surrounding a zone without FMISO uptake. The high uptake disappeared during the chronic phase, indicating that the FMISO-positive tissue had either infarcted or recovered. These results were confirmed in a larger study by Read *et al.* in 1998[37]: in 9 cases, FMISO-trapping was detected 6.25–42.5 h after stroke onset, but was absent in later examinations. Tissue with increased FMISO uptake was usually present in the periphery of the infarct identified on the co-registered late CT, but extended into normal tissue adjacent to the infarct in a few cases. The volume of tissue with increased FMISO uptake declined after stroke onset. The proportions of hypoxic tissue that infarcted or survived varied between patients. Within 6 h of stroke onset, ~90% of the FMISO-positive region was included in the final infarct but this percentage was reduced later on[38]. In addition, the volume of initially affected tissue is correlated with the initial severity of neurologic deficits, and the proportion of initially affected tissue progressing to infarction is correlated with neurological deterioration during the first week after stroke[39].

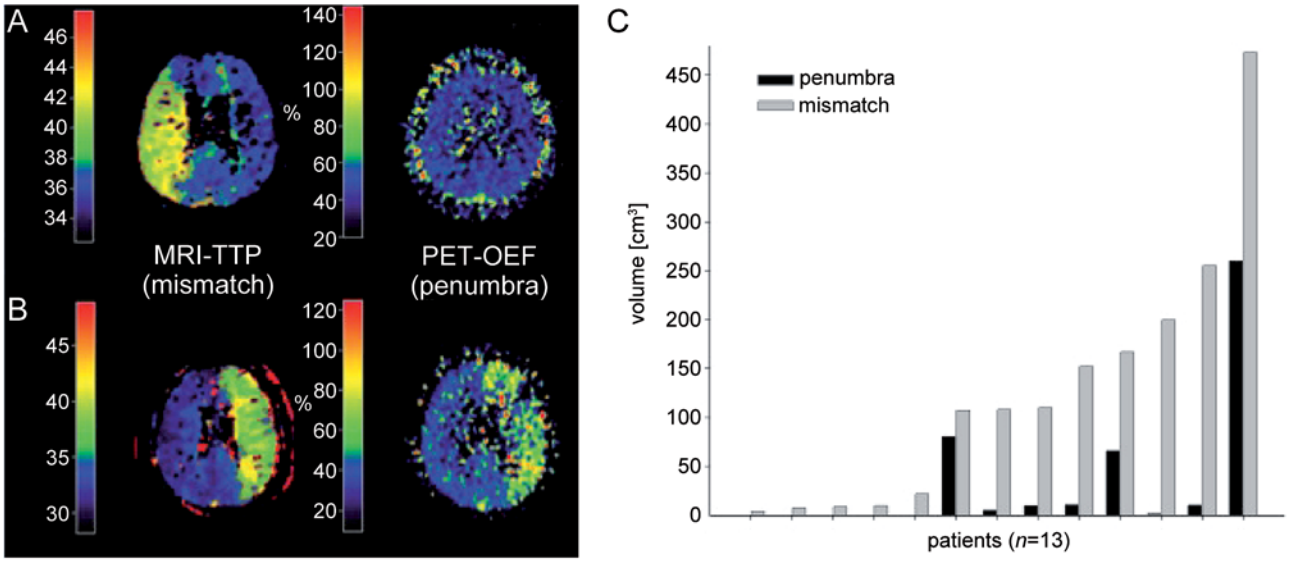

Fig. 3. A, B: Volumetric comparison of time-to-peak (TTP) (MRI) and OEF (PET) images in 2 patients in the chronic phase of stroke. In both patients, a TTP delay of 4 s indicates a considerable mismatch volume (red contour on TTP images). The mismatch volumes were 473 cm^3 for patient A and 199.7 cm^3 for patient B. However, only patient B had a corresponding volume of penumbra (260 cm^3). C: Volumes of penumbra and mismatch defined by TTP >4 s in 13 patients. All 13 showed mismatch, but only 8 showed a penumbra, which comprised 1–75% of the mismatch volume (modified from Sobesky J *et al.*, Stroke 2005[28]).

As high FMISO uptake in these areas fulfills the definition of the penumbra, the topography of FMISO-trapping can be used to generate a "penumbragram"[40].

After 2-h transient occlusion of the MCA in the rat, the area of FMISO uptake is much larger than the area of subsequent infarctions, since a variable portion of the tissue detected by FMISO uptake does not go on to infarct if untreated[41]. However, in order to provide adequate time for the washout of unbound tracer, scanning of FMISO uptake cannot be performed until 2 h after injection. In addition, due to tracer dynamics, the timing of imaging is crucial with an optimal time of 2 h for the identification of tissue at risk[42]. In permanent experimental MCA occlusion[43] and in human stroke[44], a portion of the FMISO-trapping area may lie outside the final infarct and a portion of the final infarct may not exhibit early tracer mapping, indicating that FMISO-trapping does not accurately identify preventable infarction and therefore may not be specific to the penumbra. This may indicate that the hypoxia necessary for FMISO-binding is less severe than the oxygen depletion responsible for neuronal necrosis[18]. The required delay between tracer injection and imaging (>2 h) further limits the value of FMISO for the selection of effective treatment in acute ischemic stroke.

PET as a Surrogate Marker for Treatment Efficiency

The efficacy of treatment in ischemic stroke can only be established by controlled, randomized, double-blind clinical trials, as successfully performed for thrombolysis with intravenous recombinant tissue plasminogen activator (rtPA)[45]. Such controlled trials require large groups of patients from many stroke centers, usually take a long time, and are expensive. Therefore surrogate markers may help to predict therapeutic effects in small groups of patients. Effects demonstrated with surrogate markers must be confirmed in controlled trials with sufficient patient populations. In recent years, identification of salvageable tissue by neuroimaging has attracted much interest as a surrogate marker for treatment efficiency in stroke.

The effect of thrombolysis, the only approved treatment for acute ischemic stroke, has been shown in imaging studies, in which reperfusion to penumbral tissue is associated with improvement in neurological deficits (Fig. 4): reperfusion significantly improves in rtPA-treated patients compared to controls[46]. The volume of tissue salvaged by reperfusion was determined by $H_2{}^{15}O$-PET within 3 h of stroke onset and compared with the volume of

infarction assessed on MRI 3 weeks after the stroke[47]. The percentage of voxels with an initial flow below the threshold of 12 mL/100 g/min that became re-perfused predicted the degree of clinical improvement within 3 weeks. Overall, only 22.7% of the grey matter initially perfused below the conventional threshold of critical ischemia became necrotic after thrombolytic therapy in this small sample, indicating that a considerable portion of the critically hypoperfused tissue is salvaged by this therapy. However, hypoperfused tissue can benefit from reperfusion only if cortical flumazenil-binding is not reduced below a critical value[48]. This marker identifies irreversibly damaged tissue that is not amenable to treatment.

In 34 patients with ischemic changes in >50% of the MCA territory in early cerebral CT scans, PET was performed with ^{11}C-FMZ to assess CBF and irreversible neuronal damage. Thereafter, probes for microdialysis and for measurement of intracranial pressure and tissue oxygen pressure were placed in the ipsilateral frontal lobe[53]. PET studies within 24 h after stroke identified larger volumes of ischemic core and larger volumes of irreversible neuronal damage in patients with a subsequent malignant course (i.e., edema formation with midline shift) than in patients with a benign course (Fig. 5). CBF within the ischemic core was significantly lower and the penumbra was smaller in the malignant than in the benign group. Therefore, PET may allow the prediction of malignant MCA infarction within the time window suggested for hemicraniectomy. Neuromonitoring helps to classify the clinical courses by characterizing the pathophysiological sequelae of malignant edema formation. In contrast to PET, however, it does not predict a fatal outcome early enough for the successful implementation of invasive therapies.

Microglial Activation as an Indicator of Inflammation

Microglia constitute up to 10% of the total cell population of the brain. As resident macrophages of the central nervous system (CNS), microglia phagocytose cellular debris, present foreign antigens, and are sensors of pathological events, including ischemia[54]. Microglia change from a resting to an activated state in response to CNS insults and function as phagocytes. In this activation process, they undergo a shift in their effector program by transforming their morphology, proliferating, releasing pro-inflammatory compounds, and increasing the expression of immunomodulatory surface antigens[55]. As one consequence, the translocator protein 18 kDa (TSPO), formerly known as the peripheral benzodiazepine receptor (PBR), is upregulated in the mitochondria of activated microglia and may thus serve as a biomarker of inflammation. Several radioligands have been developed to image the activation of microglia in experimental models and in various diseases of the CNS[56]. Early studies in ischemia models using ^{3}H-PK 11195 autoradiography demonstrated increased binding sites in the area of infarction and in the boundary zones between major arteries in hypertensive animals. These were associated with reactive glial cells and macrophages and reached a maximum 4–8 days after the induction of local ischemia. When high-resolution microPET was applied to the expression of TSPO/PBR in transient experimental ischemia, a high signal was detected in the ischemic core starting on day 4 and increasing to day 7, and this strong signal was associated with microglia/macrophages. A less prominent signal indicating elevated TSPO expression was observed in the region surrounding the infarct at day 7, and this could be attributed to reactive astrocytes. These results demonstrated that the cellular heterogeneity of TSPO/PBR expression depends on the intrinsic features of inflammatory cells[57, 58]. In permanent ischemia induced by microspheres injection into the MCA of rats, no increase in ^{3}H-PK 11195-binding was found in the infarct core 7 days after the attack, but the permanent MCA ischemia caused increased tracer-binding in the normoperfused peri-infarct zone, which was co-localized with increased glucose metabolism and accumulated microglia and macrophages. This peri-infarct neuroinflammation might contribute to the extension of tissue damage[59]. After temporary (45 min) MCA occlusion in hypertensive rats, significant increases in ^{11}C-PK 11195-binding in both the infarct and the surrounding areas were observed after 14 days, and less but still increased uptake was already present after 2 days[60]. With multimodal imaging including a tracer for mitochondrial complex I activity, neuronal damage is identifiable in the areas with neuroinflammation[61].

Many histological studies have identified activated microglia in the ischemic brain after stroke in humans, especially in the ischemic core within 1 to 2 days after stroke. Over time, they extend from the ischemic core into

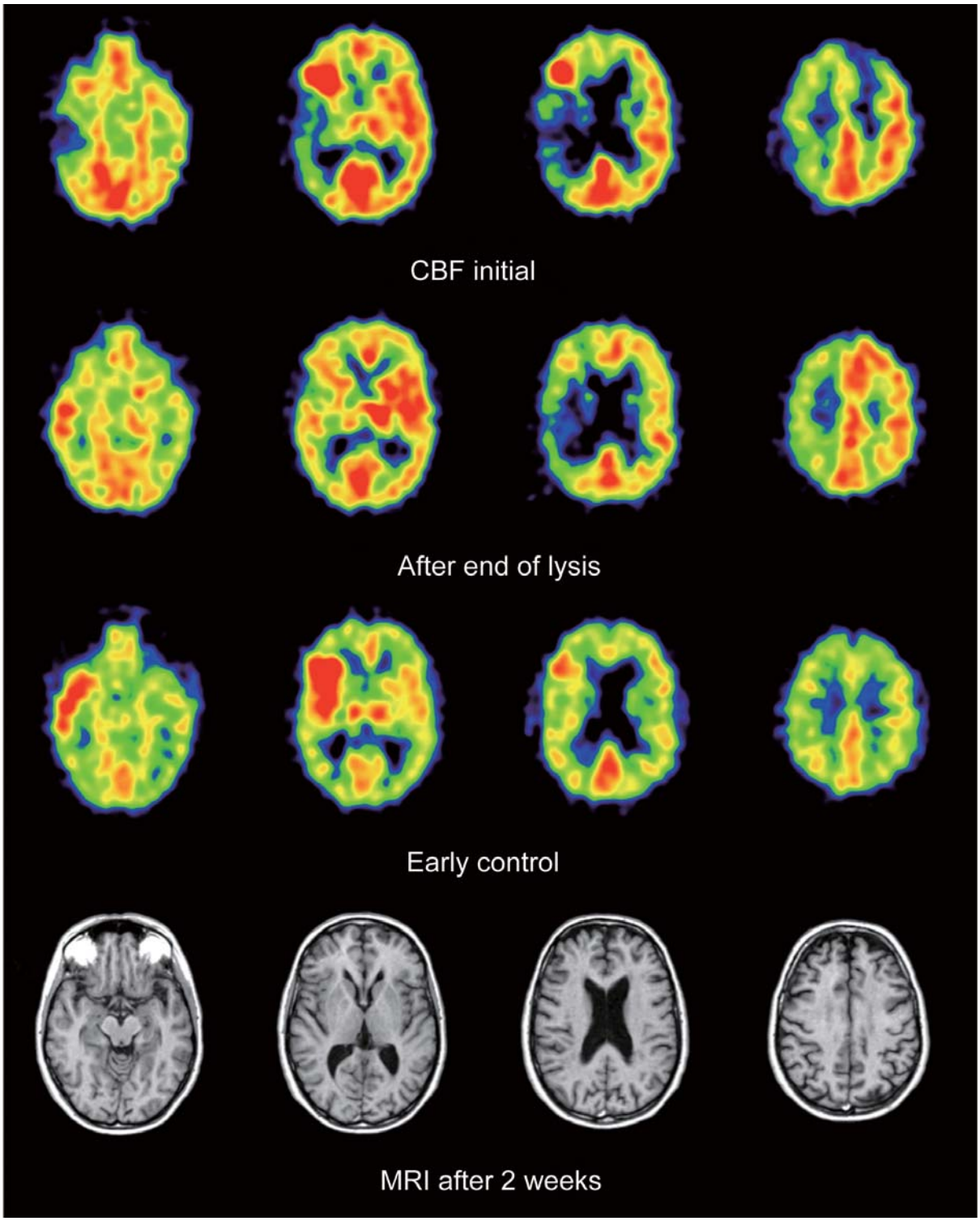

Fig. 4. Effect of thrombolysis (intravenous rTPA) in a 45-year-old woman with stroke due to multiple cerebral emboli *via* an open foramen ovale originating from deep vein thrombosis. The patient showed defects in the right MCA and left ACA territories at initial CBF PET, then lysis reperfusion was applied to both territories. Early control after 1 day showed hyperperfusion in the right MCA. MRI after 2 weeks did not indicate permanent tissue damage, indicating the patient had completely recovered.

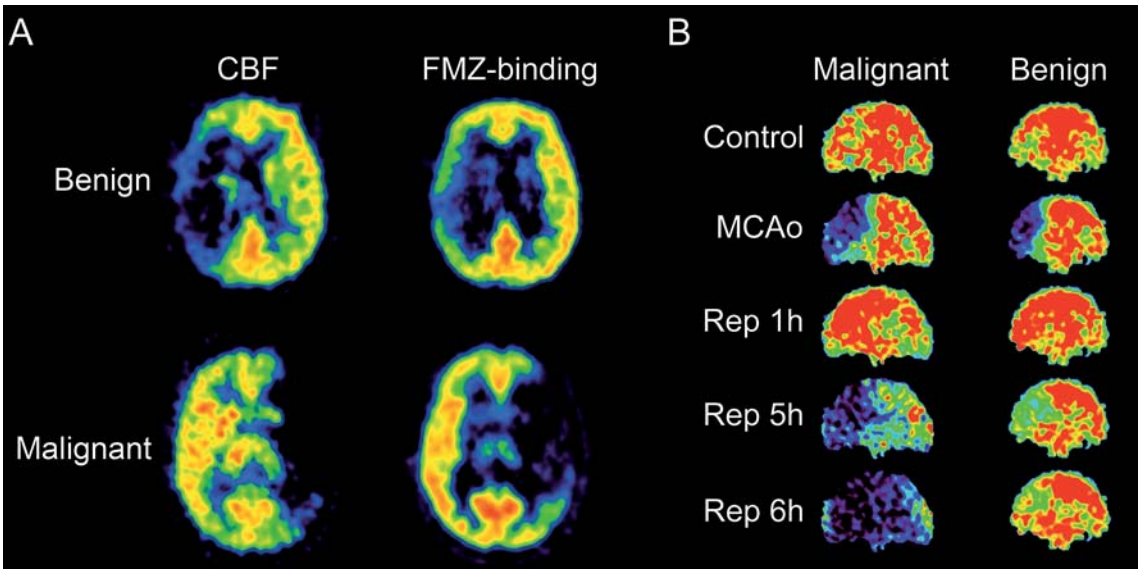

Fig. 5. Benign and malignant infarction in patients and cats (adapted from Heiss WD. Stroke 2012[19]). A: FMZ-distribution and FMZ-binding in patients with large MCA infarcts. In benign infarcts, the volumes of severe hypoperfusion and neuronal damage, i.e. reduced FMZ binding, were smaller than those in patients with a malignant course. B: Sequential PET CBF images in 2 cats with malignant (left) and benign (right) courses after transient MCA occlusion. Note the hyperperfusion immediately following recirculation and subsequent deterioration extending even to the contralateral hemisphere in the cat with malignant infarct.

the peri-infarct zones[55, 62]. In several studies, increased ^{11}C-PK11195 uptake has been observed around the ischemic lesions after several days, but also in regions distant from the lesion[56]. Increased PK-binding has also been documented in the ipsilateral thalamus and in the subcortical white matter. This relationship between neuroinflammation and the integrity of fiber tracts has been investigated more systematically by combining microglia PET with diffusion tensor imaging (DTI), which yields information about the anisotropic diffusion of water molecules along white-matter fiber tracts. Using DTI in a prospective controlled study, Radlinska *et al.*[63] demonstrated that microglial activation occurs along the pyramidal tract anterograde to the lesion only in those patients with acute subcortical stroke where the cortico-spinal tract is affected. These anterograde regions of the tract undergo Wallerian degeneration in the weeks and months after the stroke. This relationship was further investigated in a similarly-designed but longitudinal study[64], in which the extent of anterograde microglial activity in the brainstem was found to be linearly related to the extent of pyramidal tract damage (Fig. 6). This remote microglial activity is positively associated with the outcome, suggesting a neuroprotective role or repair function of microglial cells along the tract regions undergoing Wallerian degeneration. In contrast, local microglial activity in the area of the infarct is only related to persisting tract damage in the chronic phase and is correlated negatively with clinical outcome.

Hemodynamic and Metabolic Reserve

Patients with arterial occlusive disease are protected against ischemic damage to a certain extent by compensatory mechanisms, which help to prevent critical ischemia when perfusion pressure drops. In patients with uni- or bilateral carotid artery disease, PET using ^{15}O-labelled tracers[66] indicates regional vasodilatation as a focal increase in cerebral blood volume (CBV) in the respective territory, and the ratio of CBF to CBV is used as an indicator of local perfusion pressure. By calculating CBF/CBV ratio (normal value 10), the territories of patent carotids, unilateral occlusion, occlusion with contralateral stenoses, and bilateral occlusions can be discriminated. The reciprocal of the local mean vascular transit time is a

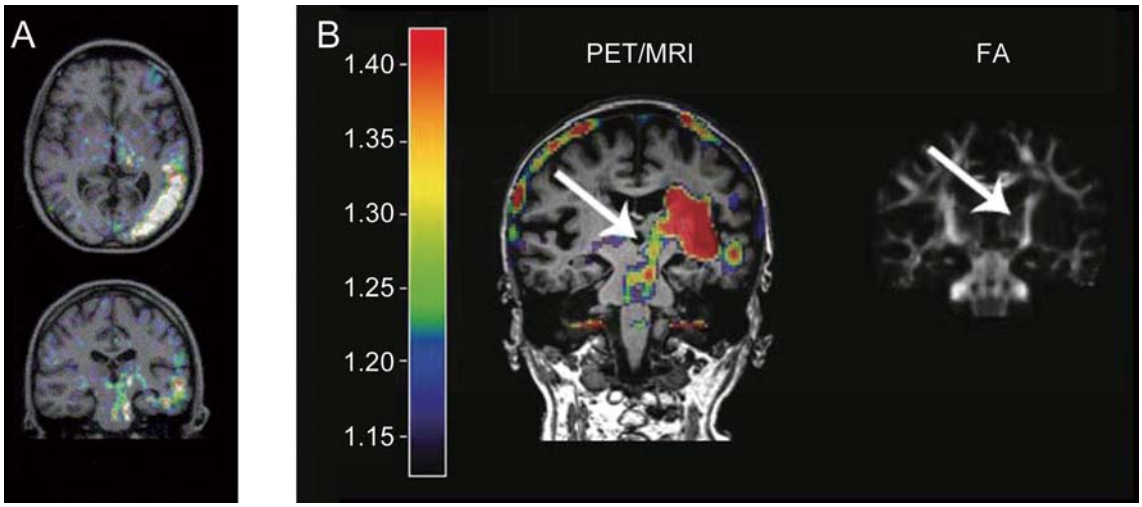

Fig. 6. Microglial activation in infarct and peri-infarct areas (A) (adapted from Gerhard A *et al.* Neuroimage 2005[62]) and in remote fiber tracts imaged by ^{11}C-PK11195-PET (B) (adapted from Thiel A *et al.* Stroke 2011[65]): ^{11}C-PK11195-PET is overlaid on T1-weigthed MRI (left) and the fractional anisotropy (FA) image shows fiber tracts (right). Tracer binding is high in the infarct but also follows the pyramidal tract (arrows) in an anterograde direction to the level of the pons. Scale indicates uptake ratios.

measure of the perfusion reserve: the lower its value, the lower the flow velocity and the longer the residence time. The lowest ratios are found in patients with symptoms indicating a hemodynamic rather than a thrombotic cause of the ischemia. At maximal vasodilatation, the perfusion reserve is exhausted and a further decrease in arterial pressure produces a proportional decrease in CBF and the CBF/CBV ratio. With this hemodynamic decompensation, the brain must draw upon the oxygen-carriage reserve to prevent energy failure and the OER is increased from the normal value of 40% to up to 85%[66-68]. Patients with submaximal elevations of OER represent 10% to 15% of the patients with cervical occlusive disease[66]; their clinical symptoms are suggestive of hemodynamic ischemia.

On the basis of such PET measurements, it is therefore possible to discriminate patients with impaired hemodynamics only, as well as to quantify the impairment of perfusion reserve, using the CBF/CBV ratio. In addition, patients who are in a more precarious physiological state can be identified because (a) their hemodynamic reserve is exhausted and (b) their focal OER is increased. These two homeostatic mechanisms seem to act in series, thereby preventing a fall in $CMRO_2$ and, hence, preventing functional disorder. Therefore, elevated OEF is an independent predictor for subsequent stroke in patients with symptomatic internal carotid artery disease, increasing the relative risk for ipsilateral stroke to ~7[69-71]. The exhausted metabolic reserve can lead to selective neuronal loss in the cortex; this cannot be detected by morphological imaging (CT or MRI) but can be documented by FMZ-PET[72]. Removal of the arterial lesion by endarterectomy or stenting is successful in preventing further ischemic attacks; repeated multiparametric PET can reveal accompanying improvements in CBF, perfusion pressure, and oxygen metabolism[73].

Deactivation of Remote Tissue (Diaschisis)

Even the earliest PET studies of ischemic brain lesions[74] revealed reduction of metabolism and blood flow exceeding the extent of morphologically damaged tissue (Fig. 7) – a regular finding since then with other functional imaging modalities as well, such as single-photon emission CT. The most conspicuous effect is a reduction of CBF and metabolism in the contralateral cerebellum, called “crossed cerebellar diaschisis” (CCD)[75], occurring immediately after a stroke and persisting permanently in patients suffering from lesions involving the cortico-ponto-cerebellar pathways, but it is reversed by successful reperfusion therapy[76](Fig. 7). This CCD is clearly due to a neuronally-

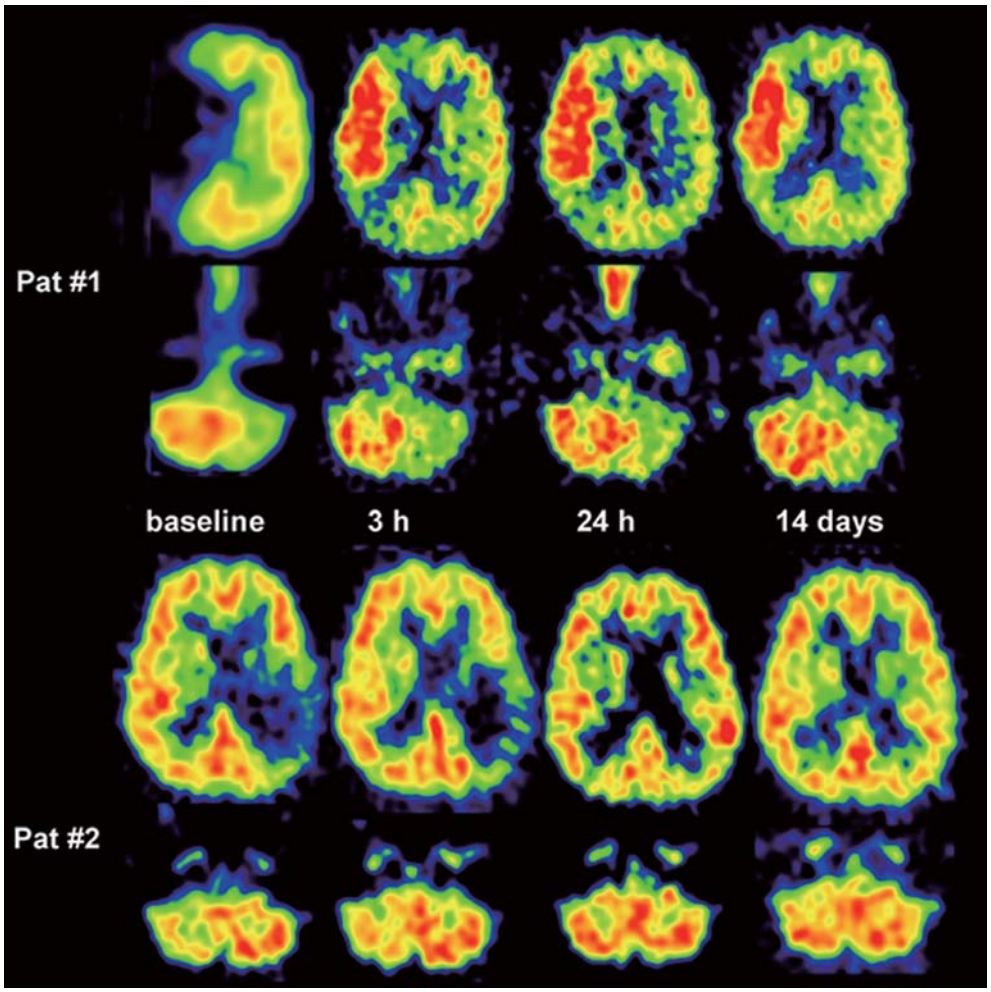

Fig. 7. Crossed cerebellar diaschisis (CCD) in acute stroke and response to supratentorial reperfusion. In patient #1, CCD persisted despite marked supratentorial reperfusion/hyperperfusion. Infarct volume was 60 cm^3, clinical outcome was poor (National Institutes of Health stroke scale (NIHSS) 9). In patient #2, supratentorial reperfusion was accompanied by a CCD decrease. Follow-up CT showed no infarct and the NIHSS outcome score was 0 (from Sobesky J *et al.* J Cereb Blood Flow Metab 2005[76]).

mediated functional effect, since a primary vascular cause can be excluded on account of the remote vascular territory. Further remote effects include reductions of CBF and metabolism in the ipsilateral cortex and basal ganglia. Their cause is less clear, since selective ischemic neuronal loss or inadequate blood supply could also contribute in these areas. However, similar effects have also been observed in non-ischemic lesions such as brain tumors and intracerebral hematomas, so they seem therefore to be more closely related to the site than to the nature of the primary lesion[77]. Among cortical and subcortical lesions, infarcts of the parietal and frontal lobes most often cause significant reductions of CBF and metabolism in the ipsilateral basal ganglia and the contralateral cerebellum. Infarcts of the basal ganglia may induce ipsilateral cerebral as well as contralateral cerebellar deactivation. Thalamic infarcts have mainly diffuse ipsilateral cortical effects; lesions of the medial thalamic nuclei apparently cause more widespread cortical metabolic reductions than those restricted to the anterior, ventrolateral, and posterior nuclei[78]. Infarcts of the brainstem and the cerebellum usually do not cause significant asymmetric inactivations of forebrain structures. It is important to note that diaschisis cannot be reliably detected by the usual PWI parameters[79].

Clinical symptoms not explained by the infarct proper can often be related to remote effects, and the severity of the metabolic changes appears to have an impact on functional recovery[80]. Especially in complex syndromes affecting parts of widespread functional networks, disturbance of a distinct function (e.g. language comprehension) is closely associated with the metabolic deactivation of a defined region (left temporo-parietal area) irrespective of infarct location[81]. Therefore, regional deactivation in specialized parts of a functional network plays a major role in the presentation of clinical syndromes and their resolution; re-organization of the affected network is of great importance for the recovery and rehabilitation of stroke victims. This complex topic is discussed in several reviews[82-85].

Vascular Dementia and Vascular Cognitive Impairment

Vascular cognitive disorders (VCDs)[86] include vascular cognitive impairment, vascular dementia (VaD, characterized by predominant deficits in executive functions and less prominent memory defects), and mixed Alzheimer VaD, and are responsible for cognitive deficits in 5% of people over the age of 65 years[87]. VCDs are heterogeneous diseases and may be caused by multiple neuropathological substrates[88, 89]. For the diagnosis of VaD and its differentiation from Alzheimer disease (AD), the presence of vascular risk factors and clinical features such as acute onset, stepwise progression, and emotional lability are used[90, 91]. In addition, neuroimaging can detect the location and extent of pathological changes related to disturbed brain function[92].

Overall, PET studies in patients with VaD demonstrate reduced CBF and $CMRO_2$, but normal OEF due to chronic ischemia[93]. In patients with large infarcts, leukoaraiosis and deep white-matter abnormalities, decreased CBF and $CMRO_2$ in the overlying grey matter are associated with the severity of cognitive impairment[94].

In VaD, fludeoxyglucose (FDG) PET shows focal cortical and subcortical hypometabolism, a pattern different from the changes in metabolism in AD (Fig. 8) affecting the association areas[95]. However, various patterns of disturbance of CBF and metabolism are observed in different conditions of vascular pathology (details in review[92]).

Post-stroke dementia (PSD) is a special case with cognitive impairment developing after the stroke, irrespective of signs of pre-existing cognitive decline. The prevalence of PSD is ~30%, i.e. 3.5 to 5.8 times greater than age-matched controls[96]. The high rate of cognitive impairment after a stroke could be caused by vascular risk factors and AD-typical metabolic changes. Clinical and experimental studies (summarized in[97]) indicate a link between vascular risk factors and degenerative dementia which is mediated by inflammation. In animal models, microglial activation after ischemia is exacerbated in the presence of amyloid and infarcts over time[98]. The processes responsible for the development of PSD can be investigated by multi-tracer PET and may serve as a basis for the development of preventive therapy.

Complex Activation Studies

Regional cerebral metabolism and blood flow are dependent on the functional state of the brain tissue. This has been well established in animal experiments using autoradiography[99]. A direct coupling of neuronal activity and focal blood flow has been demonstrated directly by simultaneous recordings with microelectrodes[100]. The transfer to human studies was achieved by the ^{133}Xenon clearance method for the measurement of regional cerebral blood flow[101], by which two-dimensional cortical activation patterns for various tasks including speech and memory were obtained. With the advance of PET, three-dimensional regional activation studies became feasible in healthy controls and in patients with various CNS disorders[102]. Due to the radiation exposure and the complex logistics required by PET, these activation studies were taken over by fMRI with the availability of high-resolution MR equipment[103]. However, PET activation studies are still required and justified for the detection of changes in the complex patterns elicited by stimulation procedures not feasible in MRI.

Our group has long experience with activation studies in aphasia[84]. In the brain of right-handers and many left-handers, language is a function of the left, dominant hemisphere. This asymmetry is established during maturation and maintained by fiber bundles connecting both hemispheres across the corpus callosum. These fibers are glutaminergic and are connected to inhibitory interneurons

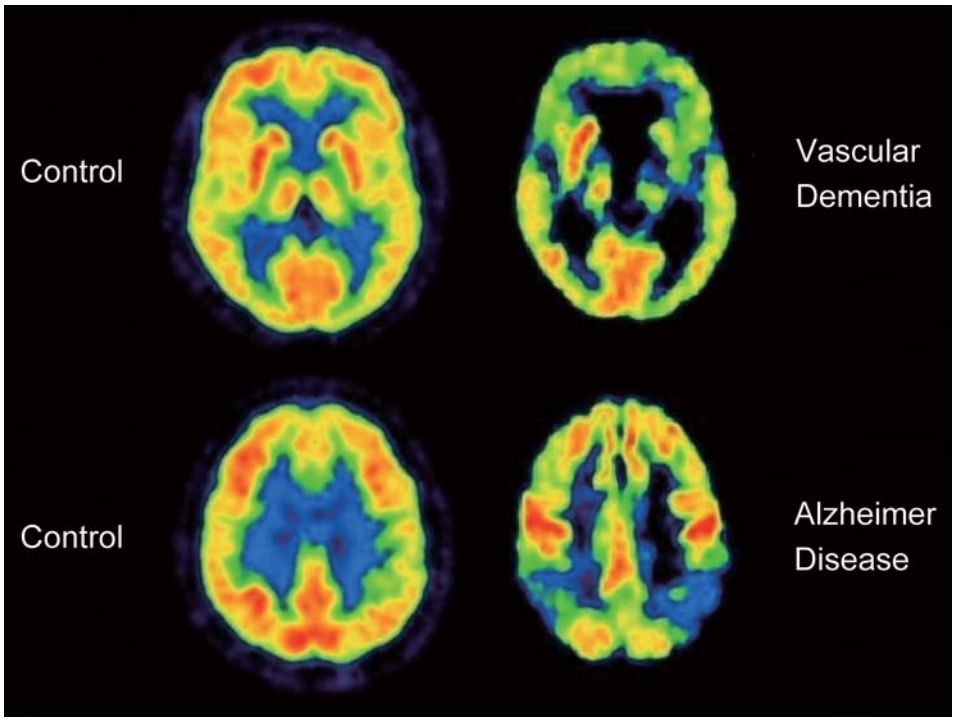

Fig. 8. Glucose metabolism in a normal control, in a patient with vascular dementia (VaD), and a patient with Alzheimer disease (AD) (Adapted from Heiss WD *et al.* J Neurol Sci 2012[92]). The severity of dementia was comparable, and the pattern of pathologic changes differentiated these two cases: patchy metabolic defects in VaD in the frontal lobe, basal ganglia, and thalamus; bilateral hypometabolism in the parieto-temporal cortex and to a lesser degree in the frontal association areas in AD.

in the non-dominant hemisphere. This means that language areas active in Broca's area suppress homologous areas in the non-dominant hemisphere (transcallosal inhibition). The existence of these inhibitory mechanisms has been deduced from imaging studies in patients with brain lesions and has been demonstrated directly in normal subjects using imaging-guided repetitive transcranial magnetic stimulation (rTMS) (Fig. 9)[104]. A lesion in the language areas of the dominant hemisphere not only reduces activity in the affected hemisphere, but also activates areas in the unaffected hemisphere by interrupting transcallosal inhibitory fibers[105]. This activity of regions in areas of the non-dominant hemisphere after a stroke has been repeatedly detected in imaging studies[106]. In the following weeks and months, activation shifts back to the dominant hemisphere. This backward shift varies considerably and might be responsible for the successful recovery of language function[107]. For successful rehabilitation, the reactivation of networks in the dominant hemisphere seems to be a more efficient strategy than recruiting homologous brain regions in the unaffected non-dominant hemisphere. Right-hemispheric regions can be compensatory in chronic aphasics[108], but this seems to be a less effective long-term strategy if left-hemisphere areas can no longer be recruited. Based on these data, a strategy for the rehabilitation of language function should suppress the right hemisphere and enhance left-hemisphere activity after stroke. Results from a study in post-stroke aphasia show that activity of the non-lesioned hemisphere can be decreased by inhibitory rTMS. The induced shift of activation to the dominant hemisphere is associated with an improvement in language function. Speech therapy combined with inhibitory rTMS of the area in the non-dominant hemisphere homologous to Broca's area might be a successful treatment for post-stroke aphasia[109].

Future Perspectives: Multimodal Imaging

With technical developments for the integration of different modalities, e.g. MRI and PET, the investigation of various

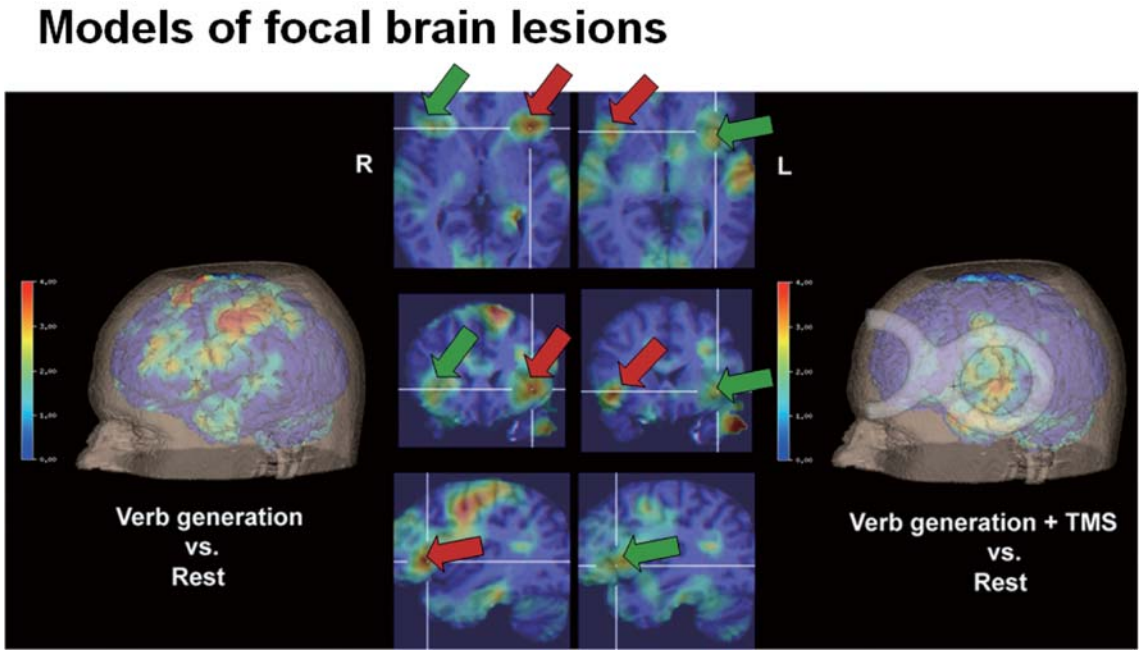

Fig. 9. Effect of repetitive transcranial magnetic stimulation on the activation pattern during verb generation. The activation pattern (left panel) and coil position (right panel) are shown in 3D rendering. Middle panels: left side, images in 3D show activation of the left inferior frontal gyrus during verb generation (red arrows); right side, decreased activation on the left (green arrows), and increased activity on the right (red arrows) during rTMS interference (modified from Thiel A *et al.* J Cereb Blood Flow Metab 2006[110]).

parameters (morphology, metabolism, blood flow and perfusion, and molecular activities) can be performed simultaneously. Combining the functional metabolic values in the picomolar range provided by PET with the fast high-resolution information in the micromolar range from MRI already has widespread applications in experimental research[111] and promising potential in humans[112-114]. The co-registration of various parameters also improves the quality of results: MR data are used for the correction of partial volume effects in small structures and dynamic information from MRI can be used for the quantification of parametric values by PET (Fig. 10).

Simultaneous multifunctional and multiparametric imaging might have a significant impact in stroke research: it guarantees exactly the same physiological state for comparative measurements of perfusion by PET and MRI; it permits differentiation of core and penumbra, demonstrates time-dependent growth of infarction, and may be used to determine the optimal therapy for a certain time after the stroke; the vascular origin of the stroke can be detected by magnetic resonance angiography, and perfusion or oxy/deoxyhemoglobin changes (the BOLD effect) can be related to the extent of oxygen deprivation (^{15}O) and hypoxia (FMISO) and to changes in metabolic markers (FDG-PET, MR spectroscopy (MRS) for lactate, choline, N-acetylaspartate) – complimentary information important for therapeutic decisions. This high-resolution anatomical information is complemented by diffusion-based tractography, and can be related to the activation or inhibition of neurotransmitter and receptor activity as well as to inflammatory reactions.

Another field of new applications may open up by combining MRS and PET. Monitoring glucose metabolism by FDG yields precise information about glycolysis. Other molecules important in glucose metabolism, such as lactate and pyruvate, can be detected by ^{13}C-MRS, which could be used together with FDG-PET to monitor different aspects of glucose metabolism in various diseases[116].

Some innovative strategies might result from the transfer of experimental findings into clinical applications of PET/MR: imaging of angiogenesis by ^{18}F-galacto RGD (a cyclic growth factor receptor peptide) combined with

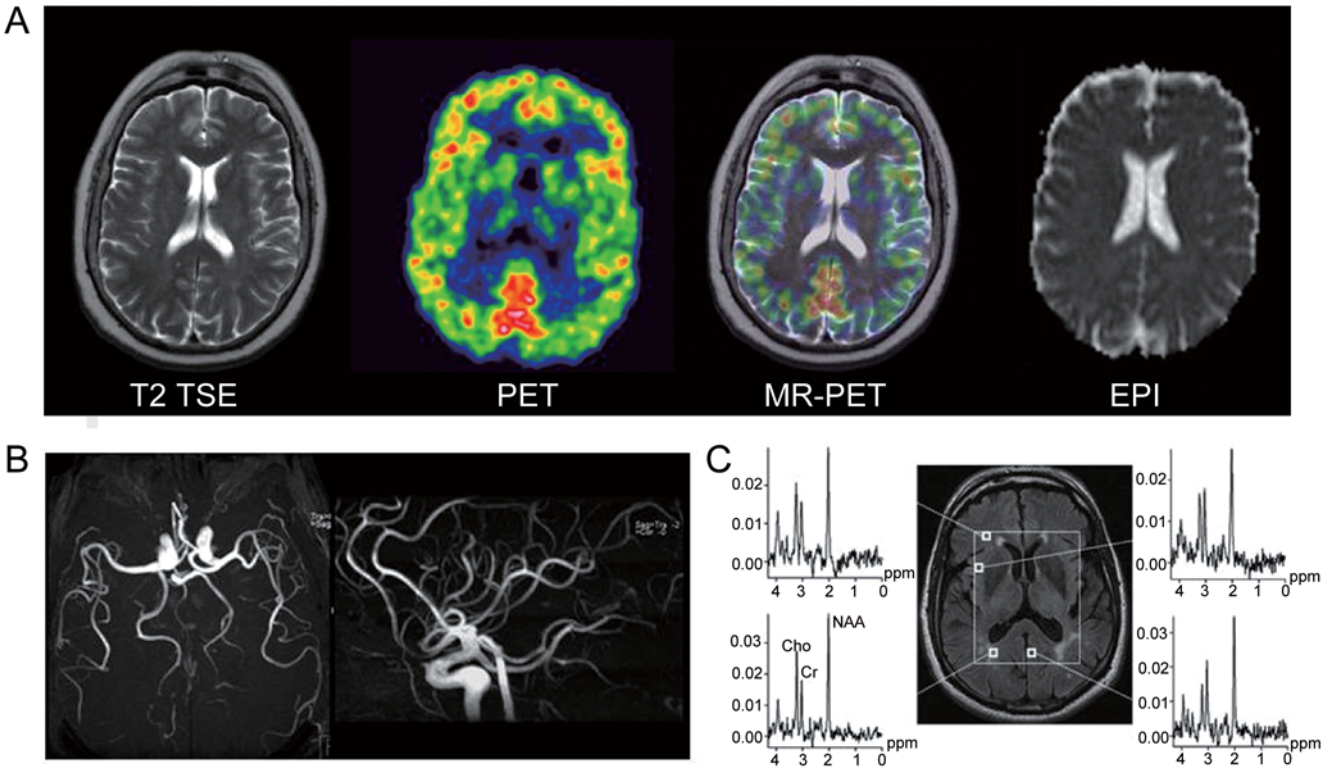

Fig. 10. The first simultaneous PET/MR acquired on the BrainPET prototype, Siemens, Knoxville, TN: Complete set of acquired MR and PET data from a 66-year-old man after injection of 370 MBq of FDG. A: T2-TSE, tracer distribution in PET recorded for 20 min at steady-state, superimposed combined PET/MR and EPI; B: time-of-flight MR-angiography; C: proton MR-spectroscopy showing increased choline relative to creatine in white matter areas (left spectra) compared to normal gray matter (right spectra) (modified from Schlemmer HP *et al.* Radiology 2008[115]).

dynamic contrast-enhanced MR might become feasible and yield information on revascularization processes in the course after stroke[117]. Monitoring the location and following the migration of grafted stem or progenitor cells will be essential in the development of cell replacement strategies for the treatment of various neurological disorders. The cells can be labelled with iron oxide particles and their survival and migration to the ischemic lesion can be followed by MRI[118]. Combining MRI for tracking cells with PET for detecting their biological activity could demonstrate the viability of the cells as well as their integration into functional networks[119, 120].

Conclusion

Over the years, PET has been the most efficient technique for providing accurate quantitative *in vivo* regional measurements of cerebral blood flow, cerebral metabolism, and cerebral molecular markers in human subjects. It therefore has played a prominent role in the translation of research concepts from experimental models to clinical application, which is fundamental for understanding the pathophysiology and for developing treatment strategies in various brain diseases including stroke. With the advent of high-resolution integrated PET/MRI facilities, simultaneous investigations of several molecular, metabolic, perfusional, and morphological parameters are feasible, and these might enhance our insights into brain function and disorders.

Received date: 2014-03-13; Accepted date: 2014-04-10

REFERENCES

[1] World Health Organisation 2008. Burden of Disease Statistics. Geneva: WHO Press.

[2] Lopez AD, Mathers CD, Ezzati M, Jamison DT, Murray CJ. Global and regional burden of disease and risk factors, 2001: systematic analysis of population health data. Lancet 2006, 367: 1747–1757.

[3] Johnston SC, Mendis S, Mathers CD. Global variation in stroke burden and mortality: estimates from monitoring, surveillance, and modelling. Lancet Neurol 2009, 8: 345–354.

[4] Leary MC, Saver JL. Annual incidence of first silent stroke in the United States: a preliminary estimate. Cerebrovasc Dis 2003, 16: 280–285.

[5] Pakkenberg B, Gundersen HJ. Neocortical neuron number in humans: effect of sex and age. J Comp Neurol 1997, 384: 312–320.

[6] Clarke DD, Sokoloff L. Circulation and energy metabolism of the brain. In: Siegel GJ, Agranoff BW, Albers RW, *et al.* (Eds.). Basic Neurochemistry: Molecular, Cellular, and Medical Aspects, 6th ed. Philadelphia: Lippincott-Raven,1999: 637–669.

[7] Sokoloff L. Energetics of functional activation in neural tissues. Neurochem Res 1999, 24: 321–329.

[8] Laughlin SB, Attwell D. The metabolic cost of neural information: from fly eye to mammalian cortex. In: Frackowiak RSI, Magistretti PI, Shulman RG, *et al.* (Eds.). Neuroenergetics: Relevance for Functional Brain Imaging. Strasbourg: HFSP Workshop XI, 2001: 54–64.

[9] Dirnagl U, Iadecola C, Moskowitz MA. Pathobiology of ischaemic stroke: an integrated view. Trends Neurosci. 1999, 22: 391–397.

[10] Hossmann KA. Pathophysiological basis of translational stroke research. Folia Neuropathol 2009, 47: 213–227.

[11] Astrup J, Siesjö BK, Symon L. Thresholds in cerebral ischemia - the ischemic penumbra. Stroke 1981, 12: 723–725.

[12] Heiss WD, Rosner G. Functional recovery of cortical neurons as related to degree and duration of ischemia. Ann Neurol 1983, 14: 294–301.

[13] Ackerman RH, Correia JA, Alpert NM, Baron JC, Gouliamos A, Grotta JC*, et al.* Positron imaging in ischemic stroke disease using compounds labeled with oxygen 15. Initial results of clinicophysiologic correlations. Arch Neurol 1981, 38: 537–543.

[14] Baron JC, Bousser MG, Comar D, Soussaline F, Castaigne P. Noninvasive tomographic study of cerebral blood flow and oxygen metabolism in vivo. Potentials, limitations, and clinical applications in cerebral ischemic disorders. Eur Neurol 1981, 20: 273–284.

[15] Lenzi GL, Frackowiak RSJ, Jones T. Cerebral oxygen metabolism and blood flow in human cerebral ischemic infarction. J Cereb Blood Flow Metab 1982, 2: 321–335.

[16] Powers WJ, Grubb RL, Jr., Darriet D, Raichle ME. Cerebral blood flow and cerebral metabolic rate of oxygen requirements for cerebral function and viability in humans. J Cereb Blood Flow Metab 1985, 5: 600–608.

[17] Heiss WD. Ischemic penumbra: evidence from functional imaging in man. J Cereb Blood Flow Metab 2000, 20: 1276–1293.

[18] Powers WJ, Zazulia AR. PET in cerebrovascular disease. PET Clin 2010, 5: 83106.

[19] Heiss WD. David sherman lecture 2012: the role of positron emission tomography for translational research in stroke. Stroke 2012, 43: 2520–2525.

[20] Heiss WD, Huber M, Fink GR, Herholz K, Pietrzyk U, Wagner R*, et al.* Progressive derangement of periinfarct viable tissue in ischemic stroke. J Cereb Blood Flow Metab 1992, 12: 193–203.

[21] Baron JC. Mapping the ischaemic penumbra with PET: implications for acute stroke treatment. Cerebrovasc Dis 1999, 9: 193–201.

[22] Graf R, Löttgen J, Ohta K, Wagner R, Rosner G, Pietrzyk U*, et al.* Dynamics of postischemic perfusion following transient MCA occlusion in cats determined by sequential PET. J Cereb Blood Flow Metab 1997, 17, Suppl. 1: S323.

[23] Guadagno JV, Jones PS, Aigbirhio FI, Wang D, Fryer TD, Day DJ*, et al.* Selective neuronal loss in rescued penumbra relates to initial hypoperfusion. Brain 2008, 131: 2666–2678.

[24] Barber PA, Darby DG, Desmond PM, Yang Q, Gerraty RP, Jolley D*, et al.* Prediction of stroke outcome with echoplanar perfusion-weighted and diffusion-weighted MRI. Neurology 1998, 51: 418–426.

[25] Kidwell CS, Alger JR, Saver JL. Beyond mismatch: evolving paradigms in imaging the ischemic penumbra with multimodal magnetic resonance imaging. Stroke 2003, 34: 2729–2735.

[26] Heiss WD, Sobesky J, Smekal U, Kracht LW, Lehnhardt FG, Thiel A*, et al.* Probability of cortical infarction predicted by flumazenil binding and diffusion-weighted imaging signal intensity: a comparative positron emission tomography/ magnetic resonance imaging study in early ischemic stroke. Stroke 2004, 35: 1892–1898.

[27] Kane I, Carpenter T, Chappell F, Rivers C, Armitage P, Sandercock P*, et al.* Comparison of 10 different magnetic resonance perfusion imaging processing methods in acute ischemic stroke: effect on lesion size, proportion of patients with diffusion/perfusion mismatch, clinical scores, and radiologic outcomes. Stroke 2007, 38: 3158–3164.

[28] Sobesky J, Weber OZ, Lehnhardt FG, Hesselmann V, Neveling M, Jacobs A*, et al.* Does the mismatch match the penumbra? Magnetic resonance imaging and positron emission tomography in early ischemic stroke. Stroke 2005, 36: 980–985.

[29] Takasawa M, Jones PS, Guadagno JV, Christensen S,

Fryer TD, Harding S*, et al.* How reliable is perfusion MR in acute stroke? Validation and determination of the penumbra threshold against quantitative PET. Stroke 2008, 39: 870–877.

[30] Zaro-Weber O, Moeller-Hartmann W, Heiss WD, Sobesky J. The performance of MRI-based cerebral blood flow measurements in acute and subacute stroke compared with 15O-water positron emission tomography: identification of penumbral flow. Stroke 2009, 40: 2413–2421.

[31] Olivot JM, Albers GW. Diffusion-perfusion MRI for triaging transient ischemic attack and acute cerebrovascular syndromes. Curr Opin Neurol 2011, 24: 44–49.

[32] Hernandez DA, Bokkers RP, Mirasol RV, Luby M, Henning EC, Merino JG*, et al.* Pseudocontinuous arterial spin labeling quantifies relative cerebral blood flow in acute stroke. Stroke 2012, 43: 753–758.

[33] Campbell BC, Christensen S, Levi CR, Desmond PM, Donnan GA, Davis SM*, et al*. Cerebral blood flow is the optimal CT perfusion parameter for assessing infarct core. Stroke 2011, 42: 3435–3440.

[34] Mathias CJ, Welch MJ, Kilbourn MR, Jerabek PA, Patrick TB, Raichle ME*, et al.* Radiolabeled hypoxic cell sensitizers: Tracers for assessment of ischemia. Life Sci 1987, 41: 199–206.

[35] Hoffman JM, Rasey JS, Spence AM, Shaw DW, Krohn KA. Binding of the hypoxia tracer [3 H]misonidazole in cerebral ischemia. Stroke 1987, 18: 168–176.

[36] Yeh SH, Liu RS, Hu HH, et al. Ischemic penumbra in acute stroke: demonstration by PET with fluorine-18 fluoromisonidazole. J Nucl Med 1994, 35: 205P.

[37] Read SJ, Hirano T, Abbott DF, Sachinidis JI, Tochon-Danguy HJ, Chan JG*, et al.* Identifying hypoxic tissue after acute ischemic stroke using PET and 18F-fluoromisonidazole. Neurology 1998, 51: 1617–1621.

[38] Markus R, Reutens DC, Kazui S, Read S, Wright P, Chambers BR*, et al.* Topography and temporal evolution of hypoxic viable tissue identified by 18F-fluoromisonidazole positron emission tomography in humans after ischemic stroke. Stroke 2003, 34: 2646–2652.

[39] Read SJ, Hirano T, Abbott DF, Markus R, Sachinidis JI, Tochon-Danguy HJ*, et al.* The fate of hypoxic tissue on 18F-fluoromisonidazole PET after ischemic stroke. Ann Neurol 2000, 48: 228–235.

[40] Markus R, Donnan G, Kazui S, Read S, Reutens D. Penumbral topography in human stroke: methodology and validation of the 'Penumbragram'. Neuroimage 2004, 21: 1252–1259.

[41] Saita K, Chen M, Spratt NJ, Porritt MJ, Liberatore GT, Read SJ*, et al.* Imaging the ischemic penumbra with 18F-fluoromisonidazole in a rat model of ischemic stroke. Stroke 2004, 35: 975–980.

[42] Spratt NJ, Donnan GA, Howells DW. Characterisation of the timing of binding of the hypoxia tracer FMISO after stroke. Brain Res 2009, 1288: 135–142.

[43] Takasawa M, Beech JS, Fryer TD, Jones PS, Ahmed T, Smith R*, et al.* Single-subject statistical mapping of acute brain hypoxia in the rat following middle cerebral artery occlusion: a microPET study. Exp Neurol 2011, 229: 251–258.

[44] Alawneh JA, Moustafa RR, Marrapu ST, Jensen-Kondering U, Morris RS, Jones PS*, et al.* Diffusion and perfusion correlates of the F-MISO PET lesion in acute stroke: pilot study. Eur J Nucl Med Mol Imaging 2014, 41: 736–744..

[45] Lees KR, Bluhmki E, von Kummer R, Brott TG, Toni D, Grotta JC*, et al.* Time to treatment with intravenous alteplase and outcome in stroke: an updated pooled analysis of ECASS, ATLANTIS, NINDS, and EPITHET trials. Lancet 2010, 375: 1695–1703.

[46] Grotta JC, Alexandrov AV. tPA-associated reperfusion after acute stroke demonstrated by SPECT. Stroke 1998, 29: 429–432.

[47] Heiss WD, Grond M, Thiel A, von Stockhausen HM, Rudolf J, Ghaemi M*, et al.* Tissue at risk of infarction rescued by early reperfusion: a positron emission tomography study in systemic recombinant tissue plasminogen activator thrombolysis of acute stroke. J Cereb Blood Flow Metab 1998, 18: 1298–1307.

[48] Heiss WD, Kracht L, Grond M, Rudolf J, Bauer B, Wienhard K*, et al*. Early [11C]Flumazenil/H_2O positron emission tomography predicts irreversible ischemic cortical damage in stroke patients receiving acute thrombolytic therapy. Stroke 2000, 31: 366–369.

[49] Hossmann KA. Pathophysiology and therapy of experimental stroke. Cell Mol Neurobiol 2006, 26: 1057–1083.

[50] Nakamura H, Strong AJ, Dohmen C, Sakowitz OW, Vollmar S, Sue M*, et al.* Spreading depolarizations cycle around and enlarge focal ischaemic brain lesions. Brain 2010, 133: 1994–2006.

[51] Dohmen C, Sakowitz OW, Fabricius M, Bosche B, Reithmeier T, Ernestus RI*, et al*. Spreading depolarizations occur in human ischemic stroke with high incidence. Ann Neurol 2008, 63: 720–728.

[52] Juttler E, Bosel J, Amiri H, Schiller P, Limprecht R, Hacke W*, et al.* DESTINY II: DEcompressive Surgery for the Treatment of malignant INfarction of the middle cerebral arterY II. Int J Stroke 2011, 6: 79–86.

[53] Dohmen C, Bosche B, Graf R, Staub F, Kracht L, Sobesky J*, et al.* Prediction of malignant course in MCA infarction by PET and microdialysis. Stroke 2003, 34: 2152–2158.

[54] Hanisch UK, Kettenmann H. Microglia: active sensor and versatile effector cells in the normal and pathologic brain. Nat

Neurosci 2007, 10: 1387–1394.

[55] Weinstein JR, Koerner IP, Moller T. Microglia in ischemic brain injury. Future Neurol 2010, 5: 227–246.

[56] Thiel A, Heiss WD. Imaging of microglia activation in stroke. Stroke 2011, 42: 507–512.

[57] Rojas S, Martin A, Arranz MJ, Pareto D, Purroy J, Verdaguer E*, et al.* Imaging brain inflammation with [(11)C]PK11195 by PET and induction of the peripheral-type benzodiazepine receptor after transient focal ischemia in rats. J Cereb Blood Flow Metab 2007, 27: 1975–1986.

[58] Demerle-Pallardy C, Duverger D, Spinnewyn B, Pirotzky E, Braquet P. Peripheral type benzodiazepine binding sites following transient forebrain ischemia in the rat: effect of neuroprotective drugs. Brain Res 1991, 565: 312–320.

[59] Schroeter M, Dennin MA, Walberer M, Backes H, Neumaier B, Fink GR*, et al.* Neuroinflammation extends brain tissue at risk to vital peri-infarct tissue: a double tracer [11C]PK11195- and [18F]FDG-PET study. J Cereb Blood Flow Metab 2009, 29: 1216–1225.

[60] Hughes JL, Jones PS, Beech JS, Wang D, Menon DK, Aigbirhio FI*, et al.* A microPET study of the regional distribution of [11C]-PK11195 binding following temporary focal cerebral ischemia in the rat. Correlation with post mortem mapping of microglia activation. Neuroimage 2012, 59: 2007–2016.

[61] Tsukada H, Ohba H, Nishiyama S, Kanazawa M, Kakiuchi T, Harada N. PET imaging of ischemia-induced impairment of mitochondrial complex I function in monkey brain. J Cereb Blood Flow Metab 2014, 34: 708–714

[62] Gerhard A, Schwarz J, Myers R, Wise R, Banati RB. Evolution of microglial activation in patients after ischemic stroke: a [11C](R)-PK11195 PET study. Neuroimage 2005, 24: 591–595.

[63] Radlinska BA, Ghinani SA, Lyon P, Jolly D, Soucy JP, Minuk J*, et al.* Multimodal microglia imaging of fiber tracts in acute subcortical stroke. Ann Neurol 2009, 66: 825–832.

[64] Thiel A, Radlinska BA, Paquette C, Sidel M, Soucy JP, Schirrmacher R*, et al.* The temporal dynamics of poststroke neuroinflammation: a longitudinal diffusion tensor imaging-guided PET study with ^{11}C-PK11195 in acute subcortical stroke. J Nucl Med 2010, 51: 1404–1412.

[65] Thiel A, Heiss W-D. Imaging of microglia activation in stroke. Stroke 2011, 42: 507–512.

[66] Gibbs JM, Wise RJ, Leenders KL, Jones T. Evaluation of cerebral perfusion reserve in patients with carotid-artery occlusion. Lancet 1984, 1: 310–314.

[67] Powers WJ, Press GA, Grubb RL, Jr., Gado M, Raichle ME. The effect of hemodynamically significant carotid artery disease on the hemodynamic status of the cerebral circulation. Ann Intern Med 1987, 106: 27–35.

[68] Sette G, Baron JC, Mazoyer B, Levasseur M, Pappata S, Crouzel C. Local brain haemodynamics and oxygen metabolism in cerebrovascular disease. Positron emission tomography. Brain 1989, 112: 931–951.

[69] Grubb RL, Jr., Derdeyn CP, Fritsch SM, Carpenter DA, Yundt KD, Videen TO*, et al.* Importance of hemodynamic factors in the prognosis of symptomatic carotid occlusion. JAMA 1998, 280: 1055–1060.

[70] Yamauchi H, Fukuyama H, Nagahama Y, Nabatame H, Ueno M, Nishizawa S*, et al.* Significance of increased oxygen extraction fraction in five-year prognosis of major cerebral arterial occlusive diseases. J Nucl Med 1999, 40: 1992–1998.

[71] Hokari M, Kuroda S, Shiga T, Nakayama N, Tamaki N, Iwasaki Y. Impact of oxygen extraction fraction on long-term prognosis in patients with reduced blood flow and vasoreactivity because of occlusive carotid artery disease. Surg Neurol 2009, 71: 532-538; discussion 538, 538–539.

[72] Baron JC, Yamauchi H, Fujioka M, Endres M. Selective neuronal loss in ischemic stroke and cerebrovascular disease. J Cereb Blood Flow Metab 2014, 34: 2–18.

[73] Matsubara S, Moroi J, Suzuki A, Sasaki M, Nagata K, Kanno I*, et al*. Analysis of cerebral perfusion and metabolism assessed with positron emission tomography before and after carotid artery stenting. Clinical article. J Neurosurg 2009, 111: 28–36.

[74] Kuhl DE, Phelps ME, Kowell AP, Metter EJ, Selin C, Winter J. Effects of stroke on local cerebral metabolism and perfusion: Mapping by emission computed tomography of ^{18}FDG and $^{13}NH_3$. Ann Neurol 1980, 8: 47–60.

[75] Baron JC, Bousser MG, Comar D, Castaigne P. "Crossed cerebellar diaschisis" in human supratentorial brain infarction. Trans Am Neurol Assoc 1980, 105: 459–461.

[76] Sobesky J, Thiel A, Ghaemi M, Hilker RH, Rudolf J, Jacobs AH*, et al.* Crossed cerebellar diaschisis in acute human stroke: a PET study of serial changes and response to supratentorial reperfusion. J Cereb Blood Flow Metab 2005, 25: 1685–1691.

[77] Feeney DM, Baron JC. Diaschisis. Stroke 1986, 17: 817–830.

[78] Szelies B, Herholz K, Pawlik G, Karbe H, Hebold I, Heiss WD. Widespread functional effects of discrete thalamic infarction. Arch Neurol 1991, 48: 178–182.

[79] Madai VI, Altaner A, Stengl KL, Zaro-Weber O, Heiss WD, von Samson-Himmelstjerna FC*, et al.* Crossed cerebellar diaschisis after stroke: can perfusion-weighted MRI show functional inactivation? J Cereb Blood Flow Metab 2011, 31: 1493–1500.

[80] Kushner M, Reivich M, Fieschi C, Silver F, Chawluk J, Rosen M*, et al.* Metabolic and clinical correlates of acute ischemic infarction. Neurology 1987, 37: 1103–1110.

[81] Karbe H, Herholz K, Szelies B, Pawlik G, Wienhard K, Heiss WD. Regional metabolic correlates of Token test results in cortical and subcortical left hemispheric infarction. Neurology 1989, 39: 1083–1088.

[82] Nudo RJ. Mechanisms for recovery of motor function following cortical damage. Curr Opin Neurobiol 2006, 16: 638–644.

[83] Mountz JM. Nuclear medicine in the rehabilitative treatment evaluation in stroke recovery. Role of diaschisis resolution and cerebral reorganization. Eura Medicophys 2007, 43: 221–239.

[84] Heiss WD. WSO Leadership in Stroke Medicine Award Lecture Vienna, September 26, 2008: Functional imaging correlates to disturbance and recovery of language function. Int J Stroke 2009, 4: 129–136.

[85] Cramer SC, Nudo RJ (Eds.). Brain Repair after Stroke. Cambridge: Cambridge University Press, 2010.

[86] Roman GC, Sachdev P, Royall DR, Bullock RA, Orgogozo JM, Lopez-Pousa S*, et al.* Vascular cognitive disorder: a new diagnostic category updating vascular cognitive impairment and vascular dementia. J Neurol Sci 2004, 226: 81–87.

[87] Rockwood K, Wentzel C, Hachinski V, Hogan DB, MacKnight C, McDowell I. Prevalence and outcomes of vascular cognitive impairment. Vascular Cognitive Impairment Investigators of the Canadian Study of Health and Aging. Neurology 2000, 54: 447–451.

[88] Ferrer I. Cognitive impairment of vascular origin: Neuropathology of cognitive impairment of vascular origin. J Neurol Sci 2010, 299(1–2): 139–149

[89] Jellinger KA. The pathology of "vascular dementia": a critical update. J Alzheimers Dis 2008, 14: 107–123.

[90] Hachinski VC, Lassen NA, Marshall J. Multi-infarct dementia. A cause of mental deterioration in the elderly. Lancet 1974, 2: 207–210.

[91] Moorhouse P, Rockwood K. Vascular cognitive impairment: current concepts and clinical developments. Lancet Neurol 2008, 7: 246–255.

[92] Heiss WD, Zimmermann-Meinzingen S. PET imaging in the differential diagnosis of vascular dementia. J Neurol Sci 2012, 322: 268–273.

[93] Frackowiak RSJ, Pozzilli C, Legg NJ, Du Boulay GH, Marshall J, Lenzi GL*, et al.* Regional cerebral oxygen supply and utilization in dementia. A clinical and physiological study with oxygen-15 and positron tomograhy. Brain 1981, 104: 753–778.

[94] Meguro K, Hatazawa J, Yamaguchi T, Itoh M, Matsuzawa T, Ono S*, et al.* Cerebral circulation and oxygen metabolism associated with subclinical periventricular hyperintensity as shown by magnetic resonance imaging. Ann Neurol 1990, 28: 378–383.

[95] Benson DF, Kuhl DE, Hawkins RA, Phelps ME, Cummings JL, Tsai SY. The fluorodeoxyglucose ^{18}F scan in Alzheimer's disease and multi-infarct dementia. Arch Neurol 1983, 40: 711–714.

[96] Leys D, Henon H, Mackowiak-Cordoliani MA, Pasquier F. Poststroke dementia. Lancet Neurol 2005, 4: 752–759.

[97] Cechetto DF, Hachinski V, Whitehead SN. Vascular risk factors and Alzheimer's disease. Expert Rev Neurother 2008, 8: 743–750.

[98] Whitehead SN, Cheng G, Hachinski VC, Cechetto DF. Progressive increase in infarct size, neuroinflammation, and cognitive deficits in the presence of high levels of amyloid. Stroke 2007, 38: 3245–3250.

[99] Sokoloff L, Ingvar DH, Lassen NA. Influence of functional activity on local cerebral glucose utilization. Brain Work 1975: 385–388.

[100] Heiss WD, Turnheim M, Vollmer R, Rappelsberger P. Coupling between neuronal activity and focal blood flow in experimental seizures. Electroenceph Clin Neurophysiol 1979, 47: 396–403.

[101] Ingvar DH. Functional landscapes of the dominant hemisphere. Brain Res 1976, 107: 181–197.

[102] Phelps ME, Mazziotta JC. Positron emission tomography: Human brain function and biochemistry. Science 1985, 228: 799–809.

[103] Raichle ME. Behind the scenes of functional brain imaging: a historical and physiological perspective. Proc Natl Acad Sci U S A 1998, 95: 765–772.

[104] Thiel A, Schumacher B, Wienhard K, Gairing S, Kracht LW, Wagner R*, et al.* Direct demonstration of transcallosal disinhibition in language networks. J Cereb Blood Flow Metab 2006, 26: 1122–1127.

[105] Thiel A, Habedank B, Herholz K, Kessler J, Winhuisen L, Haupt WF*, et al.* From the left to the right: How the brain compensates progressive loss of language function. Brain Lang 2006, 98: 57–65.

[106] Saur D, Lange R, Baumgaertner A, Schraknepper V, Willmes K, Rijntjes M*, et al.* Dynamics of language reorganization after stroke. Brain 2006, 129: 1371–1384.

[107] Heiss WD, Kessler J, Thiel A, Ghaemi M, Karbe H. Differential capacity of left and right hemispheric areas for compensation of poststroke aphasia. Ann Neurol 1999, 45: 430–438.

[108] Richter M, Miltner WH, Straube T. Association between therapy outcome and right-hemispheric activation in chronic aphasia. Brain 2008, 131: 1391–1401.

[109] Thiel A, Hartmann A, Rubi-Fessen I, Anglade C, Kracht L, Weiduschat N*, et al.* Effects of noninvasive brain stimulation on language networks and recovery in early poststroke aphasia. Stroke 2013, 44: 2240–2246.

[110] Thiel A, Schumacher B, Wienhard K, Gairing S, Kracht LW, Wagner R*, et al.* Direct demonstration of transcallosal disinhibition in language networks. J Cereb Blood Flow Metab 2006, 26: 1122–1127.

[111] Wehrl HF, Judenhofer MS, Wiehr S, Pichler BJ. Pre-clinical PET/MR: technological advances and new perspectives in biomedical research. Eur J Nucl Med Mol Imaging 2009, 36: S56–68.

[112] Heiss W-D. The potential of PET/MR for brain imaging. Eur J Nucl MEd Mol Imaging 2009, 36. Suppl 1: 105–112.

[113] Sauter AW, Wehrl HF, Kolb A, Judenhofer MS, Pichler BJ. Combined PET/MRI: one step further in multimodality imaging. Trends Mol Med 2010, 16: 508–515.

[114] Catana C, Drzezga A, Heiss WD, Rosen BR. PET/MRI for neurologic applications. J Nucl Med 2012, 53: 1916–1925.

[115] Schlemmer HP, Pichler BJ, Schmand M, Burbar Z, Michel C, Ladebeck R*, et al.* Simultaneous MR/PET imaging of the human brain: Feasibility study. Radiology 2008, 248: 1028–1035.

[116] Lanfermann H, Kugel H, Heindel W, Herholz K, Heiss WD, Lackner K. Metabolic changes in acute and subacute cerebral infarctions: findings at proton MR spectroscopic imaging. Radiology 1995, 196: 203–210.

[117] Hsu AR, Chen X. Advances in anatomic, functional, and molecular imaging of angiogenesis. J Nucl Med 2008, 49: 511–514.

[118] Hoehn M, Himmelreich U, Kruttwig K, Wiedermann D. Molecular and cellular MR imaging: potentials and challenges for neurological applications. J Magn Reson Imaging 2008, 27: 941–954.

[119] Bliss T, Guzman R, Daadi M, Steinberg GK. Cell transplantation therapy for stroke. Stroke 2007, 38: 817–826.

[120] Wang J, Chao F, Han F, Zhang G, Xi Q, Li J*, et al.* PET demonstrates functional recovery after transplantation of induced pluripotent stem cells in a rat model of cerebral ischemic injury. J Nucl Med 2013, 54: 785–792.

[121] Heiss WD, Grond M, Thiel A, Ghaemi M, Sobesky J, Rudolf J, Bauer B, Wienhard K. Permanent cortical damage detected by flumazenil positron emission tomography in acute stroke. Stroke 1998, 29: 454–461.